

Inverse chemical modeling and radiocarbon dating of palaeogroundwaters: The Tertiary Ledo-Paniselian aquifer in Flanders, Belgium

W. J. M. van der Kemp¹

Faculty of Earth Sciences, Free University of Amsterdam, Amsterdam
Laboratory for Applied Geology and Hydrogeology, Ghent University, Ghent, Belgium

C. A. J. Appelo²

Faculty of Earth Sciences, Free University of Amsterdam, Amsterdam

K. Walraevens

Laboratory for Applied Geology and Hydrogeology, Ghent University, Ghent, Belgium
Fund for Scientific Research, Flanders, Belgium

Abstract. Groundwater samples from the Ledo-Paniselian aquifer have been interpreted for chemical reaction patterns, ¹⁴C age, and recharge conditions. This confined Tertiary aquifer dips NNE from its outcrop in Belgium toward the North Sea over a length of ~50 km. Conventional ¹⁴C ages of the water samples range from 3 to over 40 ka. Inverse chemical modeling was done to correct the ¹⁴C ages for the chemical reactions in the aquifer, while accounting for changes in the recharge water quality during the Holocene and late Pleistocene. The aquifer shows a zonal pattern with (going upstream) Na-, K-, NH₄-, Mg-, and Ca-HCO₃ water types. The pattern is a result of freshening: Ca displaces the saline cations Na, K, NH₄, and Mg from the aquifer's cation exchange complex in a chromatographic sequence. The loss of Ca²⁺ from solution by cation exchange is by far the most important reaction for dissolution of calcite, which increases the apparent ¹⁴C age of the water samples. The ¹⁴C age furthermore depends on open/closed conditions of calcite dissolution and CO₂ gas exchange and CO₂ pressure in the recharge area. It is shown that δ¹³C and CO₂ pressure in a soil are interrelated and that the changes in CO₂ pressure can be included in an inverse model which considers variations in infiltration water quality. The overall correction for ¹⁴C age is obtained by inverse modeling of water quality and δ¹³C, with optimization on CO₂ pressure in recharge water using PHREEQC [Parkhurst, 1995]. The optimized CO₂ pressure for the recharge area varies with age and is generally lower in the water samples with an age above 13 ka. The lower CO₂ pressure is corroborated by lower δ¹⁸O values of the water.

1. Introduction

Inverse chemical modeling of groundwater allows one to extract reaction patterns from observed water qualities in aquifers [Back *et al.*, 1984; Plummer *et al.*, 1990; Plummer, 1992; Parkhurst, 1997]. The inverse models are based on relating the concentrations in a groundwater sample to an initial water quality using a user-specified set of reactions [Plummer *et al.*, 1990, 1994; Parkhurst and Plummer, 1993; Parkhurst, 1997; Aravena *et al.*, 1995; Chapelle and McMahon, 1991]. The extents of the various reactions in the set are obtained by mole balancing [Parkhurst *et al.*, 1982; Plummer *et al.*, 1994; Parkhurst, 1995]. The initial water quality may be that of a groundwater sample upstream along a flow line in an aquifer, or it may be a guess at the water quality in the recharge area of

an aquifer which infiltrated thousands of years ago. The reactions in the aquifer are essential for correcting ¹⁴C ages of groundwater samples.

The models published so far [Plummer *et al.*, 1983, 1990; Chapelle and Knobel, 1985; Chapelle and McMahon, 1991; McMahon and Chapelle, 1991; Aravena *et al.*, 1995] have not explicitly considered how the inverse model parameters are affected by changes in recharge conditions. The climatic conditions during the late Pleistocene have varied dramatically, giving rise to a potentially large range of soil carbon dioxide pressures and associated varying circumstances for calcite dissolution. It is obvious that total inorganic carbon (TIC) of groundwater is affected by the soil conditions, but the fact that δ¹³C in soil water can also change with CO₂ pressure in the soil has not been evaluated in the inverse models. In fact, an almost linear relation exists between δ¹³C of soil gas and the inverse of soil CO₂ pressure [Cerling *et al.*, 1991]. This linear relation allows the variations in both soil CO₂ pressure and δ¹³C together to be included in the inverse model.

This paper considers how variations in initial water quality can be included in inverse models. Each postulated initial water quality will lead to another set of reactions in the aquifer.

¹Now at Sub Atomic Physics Department, Faculty of Physics and Astronomy, Utrecht University, Utrecht, Netherlands.

²Now at Amsterdam, Netherlands.

Copyright 2000 by the American Geophysical Union.

Paper number 1999WR900357.
0043-1397/00/1999WR900357\$09.00

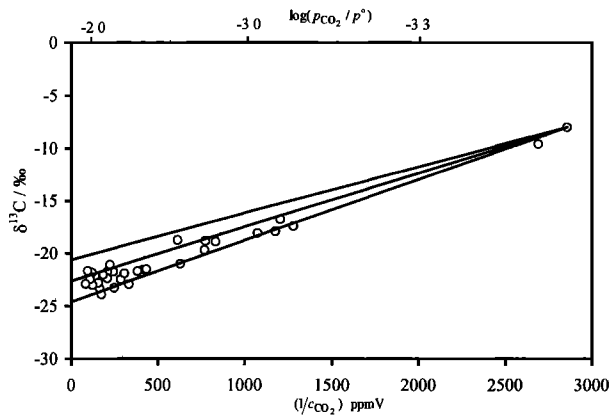


Figure 1. The $\delta^{13}\text{C}$ of soil carbon dioxide as a function of reciprocal soil carbon dioxide concentration in ppmV. Experimental data are from Dudziak and Halas [1996], Halas and Dudziak [1989], Cerling et al. [1991], and Rightmire [1978]. The lines drawn represent soil-produced CO_2 with -29 , -27 , and -25‰ . The common point represents modern atmospheric CO_2 .

The set with the minimal residual error, calculated by the inverse model PHREEQC [Parkhurst, 1995], is considered to provide the optimal description for a given water sample. It will give an optimal ^{14}C age correction and also yield information on the past recharge conditions because CO_2 pressure must be related to climatic variations. An uncertainty still resides in the choice of open versus closed models for CO_2 exchange among water, calcite, and soil gas. The ideal cases are illustrated and discussed in the paper.

The concept of inverse modeling with variable recharge water qualities was applied to data from the Ledo-Paniselian (LP) aquifer collected by Walraevens [1987]. This confined, Tertiary aquifer extends over a length of 50 km from its outcrop in Belgium toward the North Sea. The water quality in the aquifer shows zonal bands of Ca-, Mg-, NH_4^- , K-, and Na- HCO_3 waters which are a result of freshening and cation exchange [Cardenal and Walraevens, 1994; Walraevens and Cardenal, 1994]. Conventional ^{14}C ages range from 3 to over 40 ka and thus span the considerable climatic variations of the Holocene and late Pleistocene.

In this paper we discuss the basic tools that were used, that is, the relation between $\delta^{13}\text{C}$ and CO_2 pressure in the infiltration area and the reactions in the aquifer that affect $\delta^{13}\text{C}$ and ^{14}C ages. The reactions in the LP aquifer are reconstructed with the inverse chemical model PHREEQC [Parkhurst, 1995, 1997]. The reaction transfers are used to deduce ^{14}C ages of the water samples.

2. Reactions Affecting $\delta^{13}\text{C}$ and ^{14}C in Groundwater

2.1. $\delta^{13}\text{C}$ and p_{CO_2} of the Soil Atmosphere

It has been shown by Dörr and Münich [1980] that $\delta^{13}\text{C}$ of soil CO_2 is enriched in ^{13}C compared to the produced CO_2 from degradation of organic matter or root respiration, because $^{13}\text{CO}_2$ diffuses more slowly to the atmosphere than the lighter $^{12}\text{CO}_2$. The ratio of the two diffusion coefficients (D) in air leads to a fractionation factor (α) of 1.0044 [Craig, 1953],

$$\alpha_D = \frac{^{12}D}{^{13}D} = \left[\frac{M_{^{13}\text{CO}_2} M_{\text{air}}}{M_{^{13}\text{CO}_2} + M_{\text{air}}} \frac{M_{^{12}\text{CO}_2} + M_{\text{air}}}{M_{^{12}\text{CO}_2} M_{\text{air}}} \right]^{1/2} \\ = \left[\frac{45 \times 29 \cdot 44 + 29}{45 + 29 \cdot 44 \times 29} \right]^{1/2} = 1.0044, \quad (1)$$

where M stands for molecular mass.

The $\delta^{13}\text{C}$ values of soil carbon dioxide are at least 4.4‰ enriched in ^{13}C , but the enrichment can be more, depending on soil carbon dioxide pressure and atmospheric carbon dioxide pressure, as was shown by Cerling [1984] with a diffusion model. The diffusive flux of CO_2 from the soil to the atmosphere over the concentration gradient dc/dz can be written [Dörr and Münich, 1980]

$$j = \varepsilon \kappa D \left. \frac{dc}{dz} \right|_{z=0}, \quad (2)$$

where ε is the air-filled porosity, κ is a factor correcting for the tortuosity, and D is the diffusion coefficient of CO_2 in air. The production of CO_2 in the soil $P(z)$ depends on depth z and is often represented by an exponential equation [Dörr and Münich, 1980; Hesterberg and Siegenthaler, 1991; Dudziak and Halas, 1996]:

$$P(z) = P_0 \exp(-z/z_0), \quad (3)$$

where $P(z)$ decreases with increasing depth (z is positive in a downward direction, and P_0 and z_0 are constants). Following Hesterberg and Siegenthaler [1991], the CO_2 flux to the atmosphere and the CO_2 production, at steady state, can be written

$$dj/dz + P(z) = 0. \quad (4)$$

With the exponential $P(z)$ function given by (3), the differential equation (4) has the solution

$$c(z) = c_{\text{atm}} + c_1 [1 - \exp(-z/z_0)], \quad (5)$$

where $c_1 = (P_0/\varepsilon)(z_0^2/\kappa D)$ and c_{atm} is the atmospheric CO_2 concentration in ppmV.

The isotopic mass balance can be written as

$$c(z) R_{\text{soil}} = c_{\text{atm}} R_{\text{atm}} + \alpha_D c_1 R_p [1 - \exp(-z/z_0)], \quad (6)$$

where R is the isotopic ratio $^{13}\text{C}/^{12}\text{C}$ and the subscript p refers to soil-produced CO_2 . This last result can be combined with (5) to obtain

$$c(z) R_{\text{soil}} = c_{\text{atm}} R_{\text{atm}} + \alpha_D [c(z) - c_{\text{atm}}] R_p. \quad (7)$$

Rearranging, introducing delta notation, and writing $c_{\text{soil}} = c(z)$ leads to

$$\delta^{13}\text{C}_{\text{soil}} = \frac{c_{\text{atm}}(\delta^{13}\text{C}_{\text{atm}} + 1) + \alpha_D(c_{\text{soil}} - c_{\text{atm}})(\delta^{13}\text{C}_p + 1)}{c_{\text{soil}}}. \quad (8)$$

A test of (8), with experimental data from various literature sources, is shown in Figure 1. The lines drawn represent CO_2 produced with $\delta^{13}\text{C}_p$ values of -29 , -27 , and -25‰ . Note that the $\delta^{13}\text{C}$ values at the intercepts of the drawn lines with the $\delta^{13}\text{C}$ axis are 4.4‰ enriched compared to $\delta^{13}\text{C}_p$. It is evident that (8) offers an excellent approximation for the carbon 13 depletion as a function of reciprocal soil CO_2 gas concentration.

2.2. The $\delta^{13}\text{C}$ and Initial ^{14}C Activity of Recharge TIC

Three cases of evolution of $\delta^{13}\text{C}$ and ^{14}C of recharge TIC are often distinguished in a sandy unsaturated zone [Ingerson and Pearson, 1964; Pearson and Hanshaw, 1970; Deines et al., 1974; Wigley, 1975; Mook, 1972, 1976; Fontes and Garnier, 1979; Reardon et al., 1980]. If the unsaturated zone contains calcite, the chemically open system dissolution of calcite is (1) full isotopic exchange between TIC and soil CO_2 , denoted as (co,io), or (2) no isotopic exchange between TIC and soil CO_2 , denoted as (co,ic). If the unsaturated zone does not contain calcite and the aquifer does, the chemically (and isotopically) closed system dissolution of calcite in the aquifer is denoted as (cc).

2.1.1. Case (co,io). In this case, dissolved total inorganic carbon of infiltration water is determined by open system equilibration with calcite and soil carbon dioxide. The concentrations of dissolved carbon dioxide, bicarbonate, and carbonate are fixed, while the $\delta^{13}\text{C}$ of these species are determined by fractionation during exchange with the carbon dioxide from the soil atmosphere. After Deines et al. [1974] the equilibrium distribution of carbon 13 among gaseous CO_2 and aqueous H_2CO_3^* , HCO_3^- , and CO_3^{2-} can be written as

$$\alpha_{\text{CO}_2(\text{g})-\text{H}_2\text{CO}_3^*(\text{aq})} = \frac{R_{\text{CO}_2(\text{g})}}{R_{\text{H}_2\text{CO}_3^*(\text{aq})}}, \quad \alpha_{\text{CO}_2(\text{g})-\text{HCO}_3^-(\text{aq})} = \frac{R_{\text{CO}_2(\text{g})}}{R_{\text{HCO}_3^-(\text{aq})}}, \quad (9)$$

$$\alpha_{\text{CO}_2(\text{g})-\text{CO}_3^{2-}(\text{aq})} = \frac{R_{\text{CO}_2(\text{g})}}{R_{\text{CO}_3^{2-}(\text{aq})}},$$

where the α are fractionation factors, which have been reported by Mook [1994] based on data by Thode et al. [1965], Rubinson and Clayton [1969], Emrich et al. [1970], Vogel et al. [1970], and Mook et al. [1974]. Substitution of the definition of $\delta^{13}\text{C}$ in the form $R = (\delta^{13}\text{C} + 1)R_{\text{PDB}}$ leads to the $\delta^{13}\text{C}$ of the aqueous species i

$$\delta^{13}\text{C}_{i(\text{aq})} = \alpha_{\text{CO}_2(\text{g})-i(\text{aq})} (\delta^{13}\text{C}_{\text{CO}_2(\text{g})} + 1) - 1, \quad (10)$$

where i represents aqueous H_2CO_3^* , HCO_3^- , and CO_3^{2-} . $\delta^{13}\text{C}$ of recharge TIC is subsequently obtained from

$$\delta^{13}\text{C}_{\text{rw}}^{\text{co,io}} = [c_{\text{H}_2\text{CO}_3^*} \delta^{13}\text{C}_{\text{H}_2\text{CO}_3^*} + c_{\text{HCO}_3^-} \delta^{13}\text{C}_{\text{HCO}_3^-} + c_{\text{CO}_3^{2-}} \delta^{13}\text{C}_{\text{CO}_3^{2-}}] / c_{\text{rw}}, \quad (11)$$

where c_{rw} stands for the TIC concentration of the recharge water and the superscript co,io stands for chemically open and isotopically open. The initial ^{14}C activity of the recharge water $A_{\text{rw}}^{\text{co,io}}$ can be approximated with an equation analogous to (11), using fractionation constants a factor of 2 larger.

2.2.2. Case (co,ic). In the case of a chemically open but isotopically closed system, the concentrations of the chemical species are identical to the previous case. Since there is no isotopic exchange between TIC and soil CO_2 , $\delta^{13}\text{C}$ of the HCO_3^- and CO_3^{2-} -species in solution is the average of $\delta^{13}\text{C}_{\text{H}_2\text{CO}_3^*}$ (as in (11)) and $\delta^{13}\text{C}_{\text{CaCO}_3}$; as a result, $\delta^{13}\text{C}$ of TIC can be written as

$$\delta^{13}\text{C}_{\text{rw}}^{\text{co,ic}} = [c_{\text{H}_2\text{CO}_3^*} \delta^{13}\text{C}_{\text{H}_2\text{CO}_3^*} + \frac{1}{2} (c_{\text{HCO}_3^-} + c_{\text{CO}_3^{2-}}) \cdot (\delta^{13}\text{C}_{\text{H}_2\text{CO}_3^*} + \delta^{13}\text{C}_{\text{CaCO}_3})] / c_{\text{rw}}. \quad (12)$$

Assuming the ^{14}C activity for calcite to be zero, the initial ^{14}C activity of the recharge water becomes

$$A_{\text{rw}}^{\text{co,ic}} = A_{\text{H}_2\text{CO}_3^*} [c_{\text{H}_2\text{CO}_3^*} + \frac{1}{2} (c_{\text{HCO}_3^-} + c_{\text{CO}_3^{2-}})] / c_{\text{rw}}, \quad (13)$$

Table 1. Atmospheric CO_2 Concentrations and $\delta^{13}\text{C}$ Values During the Late Pleistocene and Holocene As Derived From Ice Cores

Period	c_{CO_2} , ppmV	$\delta^{13}\text{C}$, ‰
Holocene	279	-6.5
Transition	243	-6.6
Glacial	198	-6.9

Average values are from Leuenberger et al. [1992] and Marino et al. [1992].

where $A_{\text{H}_2\text{CO}_3^*}$ is the activity of H_2CO_3^* in isotopic equilibrium with soil CO_2 .

Empirical evidence indicates that $A_{\text{rw}} < 100$ percent modern carbon (pmC); according to Vogel [1970], $A_{\text{rw}} = 85 \pm 5$ pmC, while Mook [1994] suggested $A_{\text{rw}} = 65 \pm 5$ pmC for recent prebomb waters. Furthermore, the use of one of these empirical A_{rw} values requires that the $\delta^{13}\text{C}$ values of the recharge water must be corrected. This can be done by assuming partial isotopic exchange between TIC and soil carbon dioxide as in the dissolution exchange model by Mook [1972, 1976]. The initial ^{14}C activity of the recharge water A_{rw} can be approximated by

$$A_{\text{rw}} = (1 - x) A_{\text{rw}}^{\text{co,io}} + x A_{\text{rw}}^{\text{co,ic}}. \quad (14)$$

The choice of A_{rw} , at constant carbon dioxide pressure, fixes the factor x . Subsequently, $\delta^{13}\text{C}$ of the recharged water can be approximated from

$$\delta^{13}\text{C}_{\text{rw}} = (1 - x) \delta^{13}\text{C}_{\text{rw}}^{\text{co,io}} + x \delta^{13}\text{C}_{\text{rw}}^{\text{co,ic}}. \quad (15)$$

For the reverse problem, with A_{rw} unknown and $\delta^{13}\text{C}$ of the recharge water known, the factor x can be calculated from

$$x = \frac{\delta^{13}\text{C}_{\text{rw}} - \delta^{13}\text{C}_{\text{rw}}^{\text{co,io}}}{\delta^{13}\text{C}_{\text{rw}}^{\text{co,ic}} - \delta^{13}\text{C}_{\text{rw}}^{\text{co,io}}}, \quad (16)$$

and A_{rw} can be calculated from (14).

2.2.3. Case (cc). In a chemically (and isotopically) closed system, $\delta^{13}\text{C}$ of TIC can be written as

$$\delta^{13}\text{C}_{\text{rw}}^{\text{cc}} = [(c_{\text{rw}}^{\text{final}} - c_{\text{rw}}^{\text{initial}}) \delta^{13}\text{C}_{\text{CaCO}_3} + c_{\text{rw}}^{\text{initial}} \delta^{13}\text{C}_{\text{H}_2\text{CO}_3^*}] / c_{\text{rw}}^{\text{final}}, \quad (17)$$

where initial refers to equilibrium between water and soil carbon dioxide (without calcite) and final refers to equilibrium between dissolved soil carbon dioxide and calcite (without a gaseous carbon dioxide phase). The initial ^{14}C activity of the recharge water is simply

$$A_{\text{rw}}^{\text{cc}} = \frac{c_{\text{rw}}^{\text{initial}}}{c_{\text{rw}}^{\text{final}}} A_{\text{TIC}}^{\text{initial}}. \quad (18)$$

2.3. Relation Between CO_2 Pressure and $\delta^{13}\text{C}$ and ^{14}C of TIC

The aqueous concentrations of the carbon species, in the different approximations (co,io), (co,ic), and (cc), can be calculated as a function of CO_2 pressure with a chemical speciation computer program, for instance, PHREEQC, while the $\delta^{13}\text{C}$ of soil CO_2 can be estimated with (8). Atmospheric CO_2 concentrations and $\delta^{13}\text{C}$ values during the late Pleistocene and Holocene, required to do these calculations, are known from ice cores, [Leuenberger et al., 1992; Marino et al., 1992]. A summary of these data is given in Table 1. The possible range

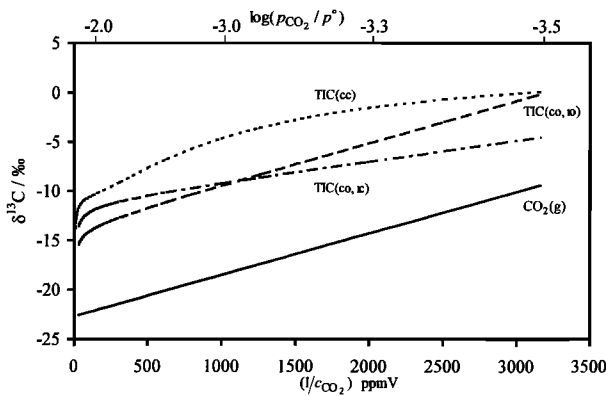


Figure 2. The $\delta^{13}\text{C}$ of soil CO_2 and recharge total inorganic carbon (TIC) as a function of reciprocal soil CO_2 concentration for soil-produced CO_2 with $\delta^{13}\text{C}_p = -27\text{‰}$. Here cc represents chemically closed system dissolution of calcite; co,io represents chemically and isotopically open system dissolution of calcite; co,ic represents chemically open and isotopically closed system dissolution of calcite.

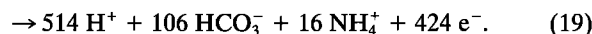
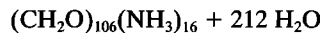
of $\delta^{13}\text{C}$ of soil CO_2 and corresponding $\delta^{13}\text{C}$ values of recharge TIC, cases (co,io), (co,ic), and (cc), are shown in Figure 2. TIC in the fully open system is 9.5‰ heavier (at 11°C) than soil gas when CO_2 pressure is smaller than 0.01 atm because of fractionation in the HCO_3^- species. At higher CO_2 pressure the H_2CO_3^* species contributes increasingly to TIC, and $\delta^{13}\text{C}$ of TIC becomes lighter. In the isotopic closed system, TIC originates half from soil CO_2 and half from calcite, with (for Figure 2) a $\delta^{13}\text{C}$ of 1.67‰. The $\delta^{13}\text{C}$ of TIC is therefore the average of the two contributions, while at higher CO_2 pressure the larger contribution of H_2CO_3^* lightens TIC again. Last, in the chemical and isotopic closed system the $\delta^{13}\text{C}$ of TIC is dominated by calcite at low CO_2 pressure; while at higher initial CO_2 pressure, it becomes grosso modo the average of the isotopic open curve and of calcite, with again some rounding due to increased importance of the H_2CO_3^* species.

The corresponding initial ^{14}C activities of recharge TIC in the different approximations are shown in Figure 3. The curves for ^{14}C can be explained similarly as for ^{13}C . TIC in the fully open system is 2 pmC enriched in ^{14}C with respect to soil gas. In the isotopic closed system, ^{14}C is the average of soil gas and dead calcite, with an increasing contribution of soil gas at higher CO_2 . In the closed system, dead carbon from calcite is the major contributor to TIC when the initial CO_2 pressure is low, and A_0 is then small.

2.4. Reactions Involving $\delta^{13}\text{C}$ in the Aquifer

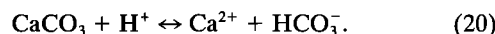
The reactions which contribute to groundwater $\delta^{13}\text{C}$ are oxidation or decomposition of organic matter and reactions of solid carbonates. Organic matter has $\delta^{13}\text{C} = -25 \pm 5\text{‰}$ in a temperate climate. Microbial oxidation of organic matter to CO_2 via O_2 , SO_4^{2-} , or Fe(III) reduction will produce CO_2 with approximately the same $\delta^{13}\text{C}$ as the organic carbon. Methane produced from organic carbon is strongly depleted and has $\delta^{13}\text{C}$ ranging from -50 to -110‰ . Methane from the marine environment is usually more depleted than methane from the freshwater environment, because the two possible methanogenic pathways, CO_2 reduction and fermentation of organic matter, proceed at a different ratio. A review considering this topic is given by Whiticar *et al.* [1986]. As methane is not

included in TIC, it follows from mass balance that TIC becomes greatly enriched upon methane production. Methane has not been reported for boreholes in the LP aquifer, and gas analysis for a number of water samples revealed no significant amounts of methane. When complications due to methanogenesis can be neglected, dissolved carbon increases according to



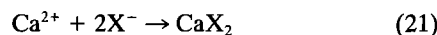
Marine carbonates show a relative isotopic enrichment in carbon 13 of -1 to 2‰ [Degens, 1967]. Dissolution will add this $\delta^{13}\text{C}$ to groundwater TIC. Dissolution occurs when acid is produced, for example, CO_2 from oxidation of organic matter, when Ca^{2+} is lost from solution, for example, by cation exchange, or when waters with different CO_2 pressures mix. Precipitation of carbonates is possible when acid is lost, for example, through reduction of SO_4^{2-} or Fe^{3+} , or when protons are exchanged, or when Ca^{2+} or other solid carbonate forming ions such as Fe^{2+} increase in concentration, for example, by cation exchange or reduction in case of Fe^{2+} . Carbon isotope fractionation between dissolved bicarbonate and precipitates is approximately 0.15‰ at 10°C [Mook, 1994] and is thus insignificant. However, it can become significant if large amounts of solid carbonates recrystallize, for instance, dissolution of dolomite and subsequent precipitation of calcite.

The relative contribution of a reaction to calcite dissolution or precipitation can be estimated in the first instance from either the protons consumed or produced or the Ca^{2+} gained or lost in the reaction:



There will be additional effects due to redistribution of the carbonate species in response to the pH changes. We give here the most common reactions.

2.4.1. Loss of calcium. Calcium may be taken up in the exchange complex



to be exchanged for other base cations

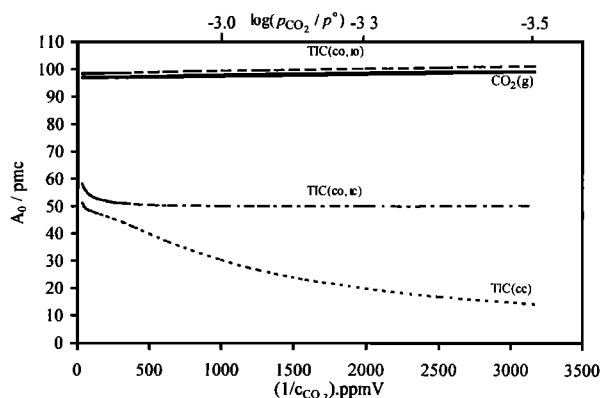
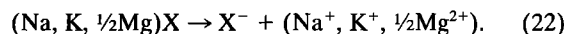
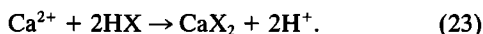


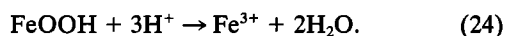
Figure 3. Initial ^{14}C activity of soil CO_2 and recharge TIC as a function of reciprocal soil CO_2 concentration for soil-produced CO_2 with $\delta^{13}\text{C}_p = -27\text{‰}$. Corrections for fractionation were made based on an initial ^{14}C activity of the atmosphere of 100‰ modern C (at $\delta^{13}\text{C} = -6.5\text{‰}$).

The loss of Ca^{2+} from solution will induce dissolution of calcite. Without proton exchange the amount which dissolves is only 10 to 20% of the Ca^{2+} loss, because pH increases when calcite releases CO_3^{2-} to the solution. Observed calcite dissolution in aquifers in response to Ca exchange can be 100% of the Ca^{2+} loss or of the Na^+ gain [Chapelle and Knobel, 1983; Plummer et al., 1994]. The amount depends on the pH buffering capacity and can be calculated for a specific solution with a forward model such as PHREEQC [Parkhurst, 1995]. The dissolution of calcite is larger than calculated for a simple (Na, K, $\frac{1}{2}\text{Mg}$) system because in the aquifer proton exchange occurs when the pH increases [Appelo, 1994],

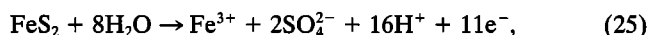


For the case of pure proton/ Ca^{2+} exchange the amount of calcite which dissolves can be calculated to be as high as 130 to 180% of Ca^{2+} loss.

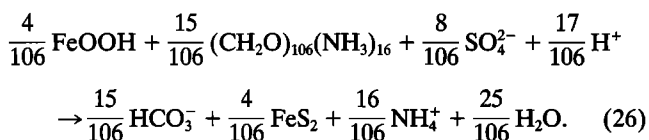
2.4.2. Combined proton/redox reactions. Protons are consumed when iron-hydroxide dissolves,



Protons are produced when pyrite oxidizes,



and when organic matter oxidizes according to reaction (19). The restriction is that in the overall reaction scheme the electrons are conserved, which allows one to deduce the net proton production. In the overall reaction, where sulfate S is reduced by organic matter and precipitates in pyrite, sulfate is replaced by bicarbonate:



The reaction shows that anions are lost, together with loss of H^+ . Replacing sulfate with the weaker acid bicarbonate will lead to further pH increase. Therefore this case of sulfate reduction by organic matter can lead to calcite precipitation.

The given reactions affect $\delta^{13}\text{C}$ of groundwater TIC, which for an aquifer in which freshwater and seawater mix, organic matter oxidizes, and calcite dissolves can be written as

$$\begin{aligned} \delta^{13}\text{C}_s = [(1 - f_{\text{sw}})c_{\text{rw}}\delta^{13}\text{C}_{\text{rw}} + f_{\text{sw}}c_{\text{sw}}\delta^{13}\text{C}_{\text{sw}} \\ + m_{\text{CaCO}_3}\delta^{13}\text{C}_{\text{CaCO}_3} + m_{\text{CH}_2\text{O}}\delta^{13}\text{C}_{\text{CH}_2\text{O}}]/c_s \end{aligned} \quad (27)$$

where f_{sw} is the seawater fraction, m the mass transfer (mmol/L), and c_{rw} and c_{sw} are the total inorganic carbon concentrations of the recharge water and seawater, respectively. Besides the chemical mass balance constraints, (27) can be used as an additional ^{13}C constraint.

2.5. Radiocarbon Dating

If no TIC altering processes take place after infiltration, then combination of the ^{14}C activity after infiltration (no decay) with the observed ^{14}C activity (with radioactive decay) leads to the ^{14}C age, ^{14}T , of a water sample:

$$^{14}T = 8270 \ln \frac{A_{\text{nd}}}{A_d}, \quad (28)$$

where the subscripts nd and d stand for no decay and decay, respectively. However, when "dead carbon" dissolves accord-

ing to the discussed reactions (equations (19), (20), and (26)), the ^{14}C activity of the sample without radioactive decay is given by

$$A_{\text{nd}} = \frac{c_{\text{rw}}}{c_s} A_{\text{rw}} \quad (29)$$

Note that the $\delta^{13}\text{C}$ correction models, usually applied, which have been reviewed by Fontes and Garnier [1979], formally cannot be used for calculating A_{nd} of the palaeowater because these models assume a constant value for $\delta^{13}\text{C}$ of soil carbon dioxide.

3. Inverse Modeling

The chemical reactions which determine water quality and their relative importance can be calculated with mass balance models or so-called inverse models [Parkhurst et al., 1982]. Originally, these models were limited in that mass transfers are constrained by the stoichiometry of the reactions, because only a set of linear equations is solved. Parkhurst [1995, 1997] has recently published a new approach which allows for inaccuracies in the analysis and for uncertainty of the reaction scheme. The uncertainty is added as a separate term (δ), and the set of reaction equations is solved with a Simplex scheme to the smallest value for δ . This enables one to (statistically) optimize the reaction scheme and to estimate the optimal parameter values in the reaction scheme.

A mass balance model which considers $\delta^{13}\text{C}$ in addition to variations in CO_2 pressure in the recharge area will enable one to deduce the amount of recharged TIC, provided that sufficient chemical and isotopic data are available to use as constraints. We have used the statistical inverse modeling approach to optimize the reaction scheme in the Ledo-Paniselian aquifer.

4. Hydrogeology and Hydrochemistry of the Ledo-Paniselian Aquifer

4.1. Hydrogeology

The Ledo-Paniselian aquifer extends from Flanders (Belgium) to Sealand (Netherlands) over a distance of ~ 100 km. The aquifer is overlain by the Bartonian clay in the recharge area and in the northern part. The aquifer becomes phreatic south of the recharge area. A map of the survey area, with sample points for hydrochemical and isotopic analyses [Walraevens, 1987], is shown in Figure 4. A schematic hydrogeological A-A' transect, indicated on Figure 4, from south to north through the recharge area southwest of Eeklo, is depicted in Figure 5. At the north end of the section the following stratigraphy is found: Quaternary sands, Boom (or Rupelian) clay, Oligocene sands, Bartoon clay, Ledo-Paniselian sands, Paniselian clay, Ypresian sands, and finally the Ypresian clay, which is taken as the impermeable bottom layer of the conceptual groundwater flow model. The Paniselian clay and the Ypresian aquifer have an average thickness of 5 and 10 m, respectively. The thicknesses of the other aquifers and aquitards vary along the transect.

Two main recharge areas exist; the most important one is situated southwest of Eeklo at a topographical high. Water infiltrates through the Bartoon clay, which locally varies in thickness between 0 and 30 m, into the Ledo-Paniselian aquifer. The other recharge area is around Sint Niklaas where

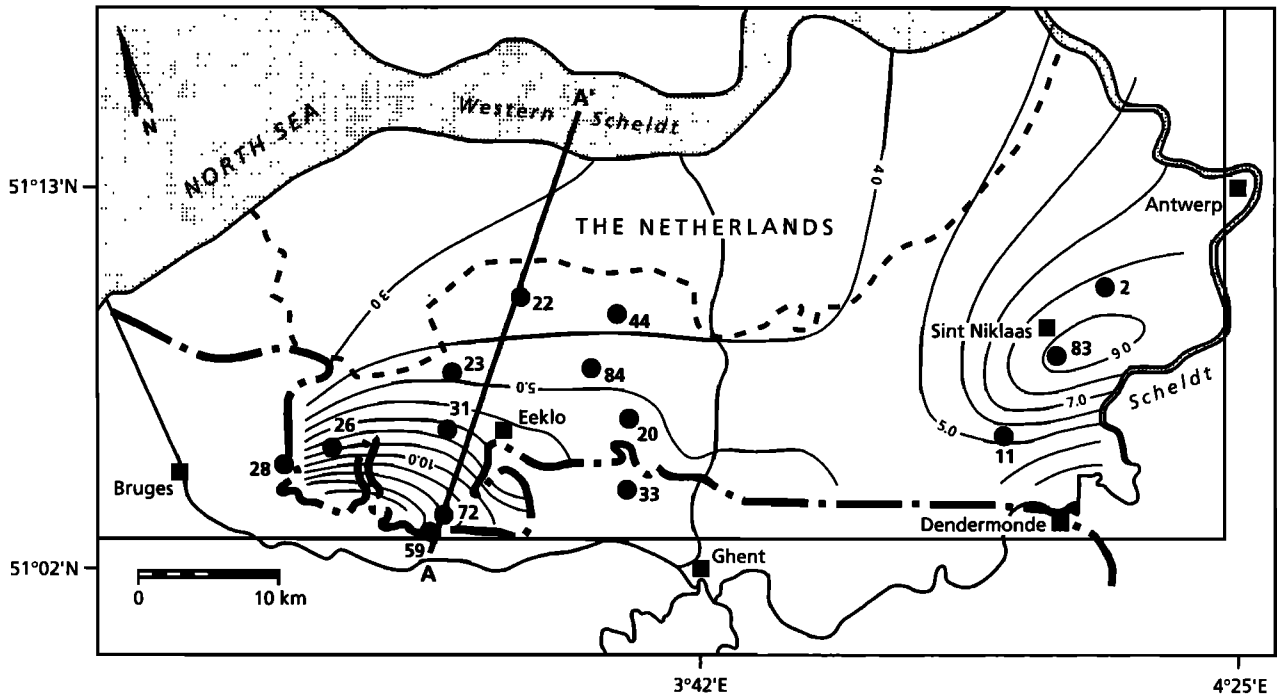


Figure 4. Map of the survey area with sampling point locations for chemical and isotopic analyses [Walraevens, 1987] and calculated hydraulic heads in the aquifer in its natural prepumping state (before 1920) [Walraevens, 1988].

recharge takes place through both the Boom clay and the Bartoon clay.

4.2. Cation Exchange and Carbonate Reactions

A sequence ranging from diluted seawater through sodium (potassium) and magnesium to calcium bicarbonate water is

observed in an upstream direction in the Ledo-Paniselian aquifer [Cardenal and Walraevens, 1994]. The pattern is closely akin to the sequence observed in the Aquia aquifer in the United States [Chapelle and Knobel, 1983; Appelo, 1994] and is the result of cation exchange reactions between aquifer sediments, equilibrated with seawater, and fresh calcium bicarbonate in-

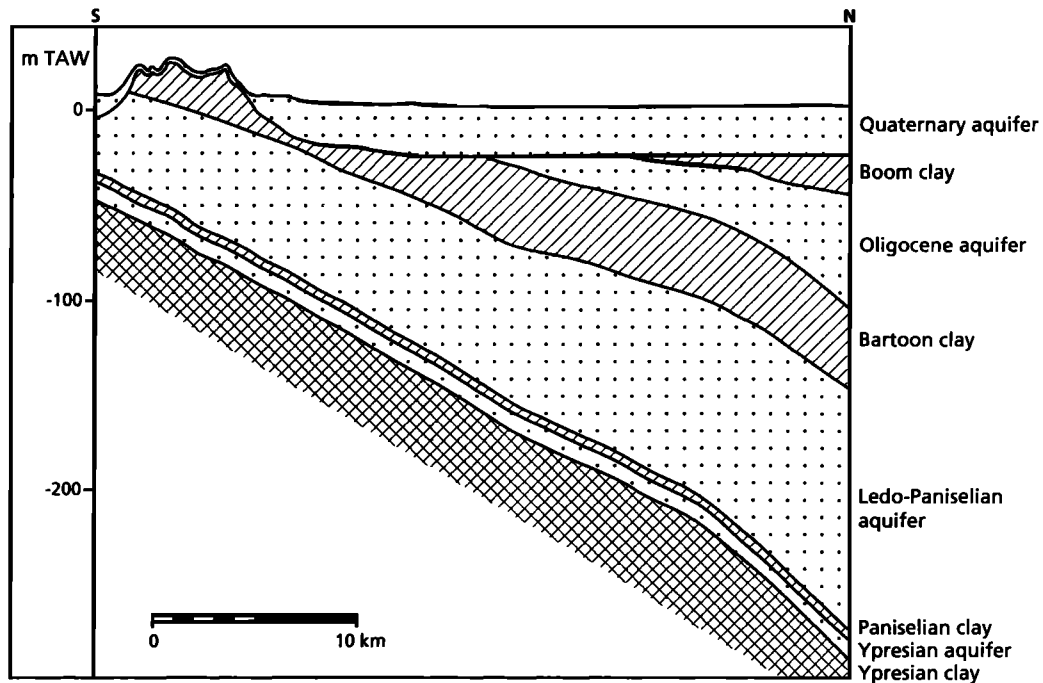


Figure 5. Hydrogeological cross section A-A' of the aquifer systems and confining units.

Table 2. Hydrochemical and Isotopic Analyses of Water Samples

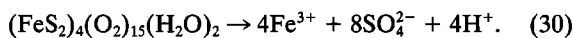
Number	pH	TIC	Alk	Ca ²⁺	Mg ²⁺	Na ⁺	K ⁺	Fe _T	NH ₄ ⁺	Cl ⁻	SO ₄ ²⁻	δ ¹³ C	¹⁴ C	δ ¹⁸ O
22	8.07	11.7	11.5	0.22	0.48	23.9	0.70	0.0144	0.0063	18.1	0.81	-2.6	2.5	-7.40
44	7.90	10.2	10.0	0.44	0.94	44.7	1.05	0.0081	0.0422	34.3	1.90	0.1	0.5	-7.03
84	8.38	11.0	11.1	0.19	0.28	13.2	0.56	0.0000	0.0111	5.37	0.31	-5.2	4.5	-7.20
20	8.02	10.6	10.5	0.31	0.42	13.0	0.69	0.0039	0.0242	3.91	0.18	-5.9	1.8	-7.00
83	8.23	12.6	12.6	0.12	0.18	24.9	0.45	0.0009	0.0000	12.4	0.34	-2.5	0.8	-7.53
11	8.59	12.9	13.2	0.07	0.11	15.0	0.38	0.0018	0.0000	3.23	0.49	-1.8	3.0	-7.06
2	8.34	10.2	10.3	0.25	0.32	38.9	0.63	0.0043	0.0000	28.2	0.44	-3.4	1.2	-7.50
26	7.48	8.30	7.69	1.61	1.17	1.96	0.69	0.0104	0.0632	0.62	0.11	-13.6	45.2	-5.57
28 _{ph}	8.31	6.20	6.19	0.20	0.24	5.22	0.42	0.0029	0.0100	0.48	0.00	-12.0	42.0	-5.50
31	7.55	6.69	6.27	1.21	1.50	1.36	0.95	0.0081	0.0742	0.57	0.58	-12.7	16.6	-6.56
72	7.60	5.68	5.38	3.29	0.72	0.65	0.26	0.0183	0.0116	0.70	1.21	-12.7	33.6	-6.51
59	7.11	5.80	4.87	3.26	0.59	1.06	0.21	0.0896	0.0269	1.21	1.39	-11.5	39.9	-6.71
23	7.75	8.33	8.01	0.91	0.65	6.45	0.75	0.0335	0.0948	3.95	0.02	-10.0	12.4	-6.99
33 _{ph}	7.18	8.52	7.31	1.26	0.28	4.57	0.29	0.0450	0.1464	0.83	0.01	-8.1	37.7	-6.40

Source is *Walraevens* [1987]. Chemical concentrations are in mmol/L. The δ¹³C and δ¹⁸O in percent mil versus Pee Dee belemnite and standard mean ocean water, respectively. The δ¹⁸O values are corrected for seawater content (seawater, δ¹⁸O = 0‰). The ¹⁴C activities are in percent modern carbon. Sample numbers with subscript ph refer to phreatic water samples. Subscript T represents total iron content.

filtration water. A chromatographic pattern develops because the cations are displaced from the saline exchanger in the order of increasing selectivity from Na⁺ first to K⁺ and NH₄⁺ and finally Mg²⁺ [Appelo, 1994].

4.3. Inverse Chemical Modeling of Water Quality in the Ledo-Paniselian Aquifer

Inverse chemical models were calculated for all samples of Table 2 with PHREEQC-2 [Parkhurst and Appelo, 1999]. PHREEQC-2 includes isotope balances in addition to the uncertainty estimates in the mass balances. Mixing between fresh recharge water (approximations (co,io), (co,ic), and (cc)) and seawater was calculated for reactions (19) to (26) and with constraints as indicated in Table 3. Furthermore, oxidation of pyrite, which occurs in the recharge area in the covering clay layer, was modeled by defining the "phase" (FeS₂)₄(O₂)₁₅(H₂O)₂. This gives rise to the reaction



Subsequently, the ferric ions can precipitate as goethite. Reaction (30) was modeled as a complete oxidation reaction to separate it from the sulfate reduction reaction (26) which may take place downstream in the aquifer. Furthermore, defining this phase and reaction, instead of a free O₂ phase, prevents the generation of models in which oxidation of organic carbon with oxygen takes place in the aquifer. The direct oxidation of organic matter in the root zone is accounted for by varying the CO₂ pressure at infiltration.

The presently available data do not permit separation of

Table 3. Mineral Phases, Exchange Species, and Constraints

	Chemical Reactants
Phases	calcite,* goethite, pyrite, (FeS ₂) ₄ (O ₂) ₁₅ (H ₂ O) ₂ ,* (CH ₂ O) ₁₀₆ (NH ₃) ₁₆ *
Exchange species	CaX ₂ , MgX ₂ , NaX, KX, NH ₄ X, and HX
Constraints	Na ⁺ , NH ₄ ⁺ , K ⁺ , Ca ²⁺ , Mg ²⁺ , Fe _T , SO ₄ ²⁻ , S ²⁻ , Cl ⁻ , TIC, Alk

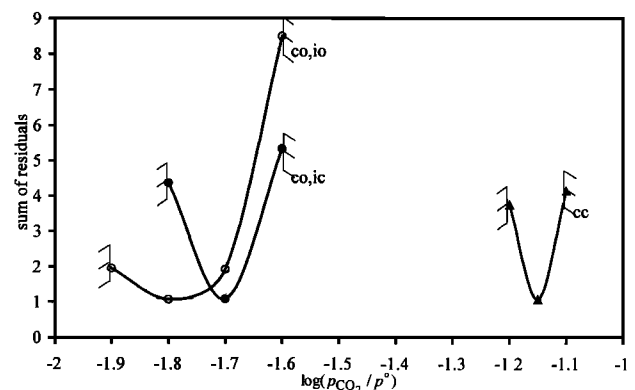
For ¹³C, seawater is 1.5 ± 0.1‰. For infiltration water, see Figure 2 (error see Figure 2). For samples see Table 2 (error ± 0.1‰). Calcite is 1.67 ± 0.5‰; organic matter is -25 ± 2‰.

*Phases may only enter the solution.

pyrite oxidation in the infiltration area according to reaction (30) and subsequent reduction of sulfate in the aquifer by reaction (26). The reduction reaction was therefore specified in the inverse model for samples with a SO₄²⁻/Cl⁻ ratio lower than seawater, while the oxidation reaction was indicated for samples with a higher ratio.

The CO₂ pressures in the recharge area were calculated for each water sample with PHREEQC-2 using steps in log p_{CO₂} of -0.1. Each CO₂ pressure gives rise to a number of models, in our case usually from 0 to 10 models. Each model is accompanied by a sum of the uncertainties generated in the input concentrations (deltas [cf. Parkhurst, 1995, 1997]). It was found that the sum of the uncertainties followed a parabola, depending on soil CO₂ pressure, and it was judged that the minimum in the curve would correspond to the optimal model for the sample.

An example of how the sum of uncertainties changes with the logarithm of soil CO₂ pressure of the infiltration water is shown in Figure 6 for sample 31. There is a break-off edge associated with each parabola which is indicated as hatched in Figure 6. Outside these edges, no models were found by PHREEQC-2 with the imposed limits for the uncertainty. The calculations were done for the three end-member cases of calcite dissolution in the recharge area for all water samples from the aquifer.

**Figure 6.** Calculated sum of residuals as a function of log pCO₂ of the infiltration water for sample 31.

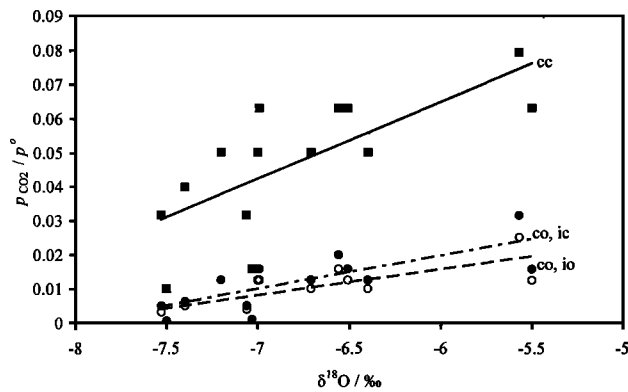


Figure 7. The $p\text{CO}_2$ at infiltration, derived from inverse chemical modeling, as a function of $\delta^{18}\text{O}$ of the water.

4.4. Results of the Inverse Model

4.4.1. CO_2 pressure in recharge water. The optimal CO_2 pressures (those associated with the lowest sum of uncertainties) are plotted as a function of $\delta^{18}\text{O}$ of the water (corrected for seawater content with $\delta^{18}\text{O} = 0\text{‰}$) in Figure 7 for the three cases of calcite dissolution in the soil discussed. All the models show that higher CO_2 pressures correlate with less negative $\delta^{18}\text{O}$, implying that warmer conditions and higher organic productivity are closely associated. It is of interest to note that the inverse modeling approach has thus provided a method to deduce palaeoclimatic conditions by separating the reactions which have contributed to the groundwater composition. Figure 7 shows that a chemically closed system for the recharge water (case cc) has a much higher initial CO_2 pressure than the two other cases. The difference between the isotopically open and closed cases is minor, which is due to the small difference in $\delta^{13}\text{C}$ of TIC in recharge water for these two cases at the model-derived CO_2 pressures (compare Figure 2). The chemically closed system requires a CO_2 pressure in the recharge area which is 5 to 10 times higher than for the open case and appears to be too high for the conditions at this

aquifer. The ratio of infiltration volume to amount of calcite present in the unsaturated zone is such that equilibrium is attained within a few centimeters of water flow in these soils. Considering the rate of dissolution of calcite under these circumstances, open system dissolution is likely [Appelo and Postma, 1993]. Therefore only the model results for the chemical and isotopic open system are considered in the following discussions.

4.4.2. Contributions to groundwater TIC. The contributions of recharge water TIC, and of reactions in the aquifer, to groundwater TIC are shown in Figure 8. The contributions are plotted against corrected ^{14}C age of the sample, which is discussed in section 4.5. The difference between analyzed groundwater TIC (indicated by circles in Figure 8) and the sum of TIC in recharge water and the dissolution of calcite in the aquifer (indicated by crosses on a continuous line) is due to organic carbon oxidation in the aquifer (triggered by sulfate reduction). Figure 8 shows that TIC in the Pleistocene samples is higher than in the Holocene waters. It also shows that the increase of TIC is a result of calcite dissolution in the aquifer, rather than in the recharge area. The amount of calcite which dissolves in the recharge area even declines in the Pleistocene samples because of the lower CO_2 pressure in the soil during the colder climatic conditions in that period, as was discussed in section 1.

The inverse model does provide the relative contributions of the reactions which trigger the dissolution of calcite in the aquifer, that is, loss of Ca^{2+} due to cation exchange and proton production due to redox reactions. The two types of reactions are plotted cumulatively versus amount of dissolved calcite in the aquifer in Figure 9. Figure 9 illustrates that calcite dissolution is due to the uptake of Ca^{2+} in the exchange complex (reaction (21)), while the combined proton/redox reactions (reactions (19), (24), and (25)) add little or nothing. The small contribution of the redox reactions in the LP aquifer also follows from the small contribution of the organic carbon oxidation reaction in the majority of the groundwater samples.

It is rather conspicuous in Figure 9 that the net amount of Ca^{2+} loss is higher than the amount of calcite which dissolves.

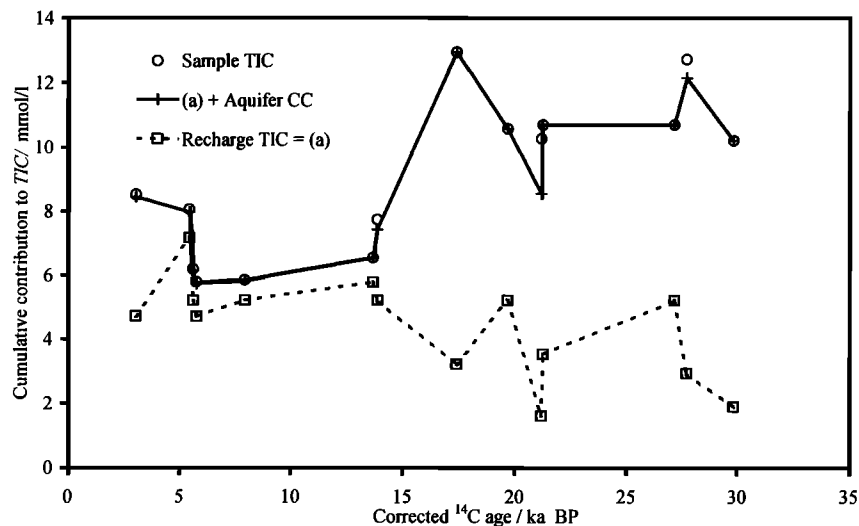


Figure 8. Comparison of contributions of recharge TIC and aquifer calcite dissolution to sample TIC as a function of the corrected radiocarbon age. The difference between sample TIC and the cumulative contribution is due to organic carbon oxidation.

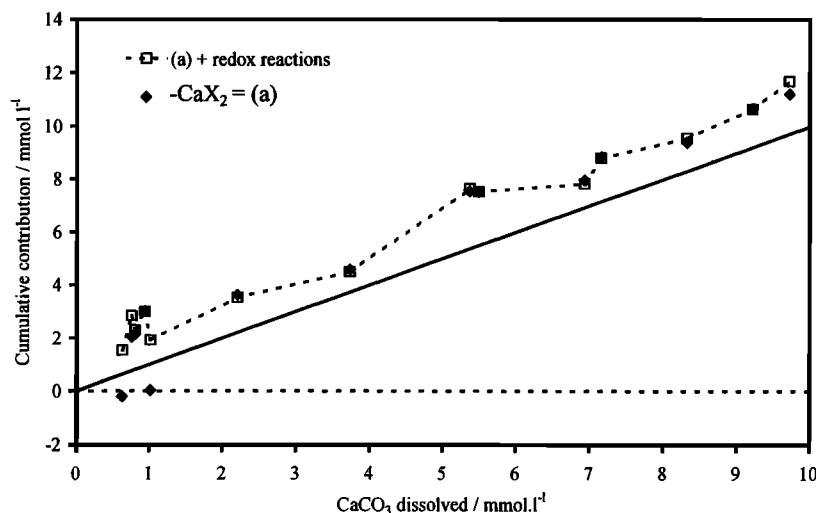


Figure 9. Cumulative plot of the contributions of cation exchange and of redox reactions to calcite dissolution in the Ledo-Paniselian aquifer. The amount of the cation exchange reaction is indicated by the diamonds (CaX_2). The redox reactions, (19), (24), and (25) in the text, are added together to the cation exchange reaction to yield the total reaction indicated by the squares. The solid line shows the 1:1 relation.

The effect is related to the pH increase which accompanies the dissolution of calcite and which requires that more calcium is removed from solution than can dissolve from calcite. The amount removed is consistently about 1 mmol/L higher for the full range of calcite dissolution from 2 to 10 mmol/L. The pH increase triggers release of protons from the exchange complex, and this accounts generally for almost half of the counter exchange against Ca^{2+} , the other half being captured by the base cations.

4.5. Radiocarbon Ages

Conventional radiocarbon dating (no corrections) of the samples shown in Table 2 leads to a maximum age >39 ka [Walraevens, 1990a, b]. The optimized inverse models, with recharge TIC (c_{rw}) as source for ^{14}C and aquifer reactions as source for dead carbon only, were used to obtain corrected radiocarbon ages with (28) and (29). The maximum ground-

water ages are found for the case of full chemical and isotopic exchange of recharge TIC with soil CO_2 , while minimum ages are obtained for the closed system. Ages derived from chemically closed system dissolution are comparable to those obtained in the chemical open case without isotopic exchange. The correction on apparent age can be as high as 15,000 years, as is illustrated in Figure 10 for the fully open case. The chemically closed system is less likely for this aquifer as discussed before.

All late Pleistocene waters in this study have measured ^{14}C activities less than 5 pmC (Figure 10), and these samples have the largest corrections on ^{14}C age. Hydrology, chloride content, and the extent of magnesium exchange can give additional clues for age determination of samples originating from the same recharge area. The samples are not generally on the same flow line, but the corrected ages for the open system

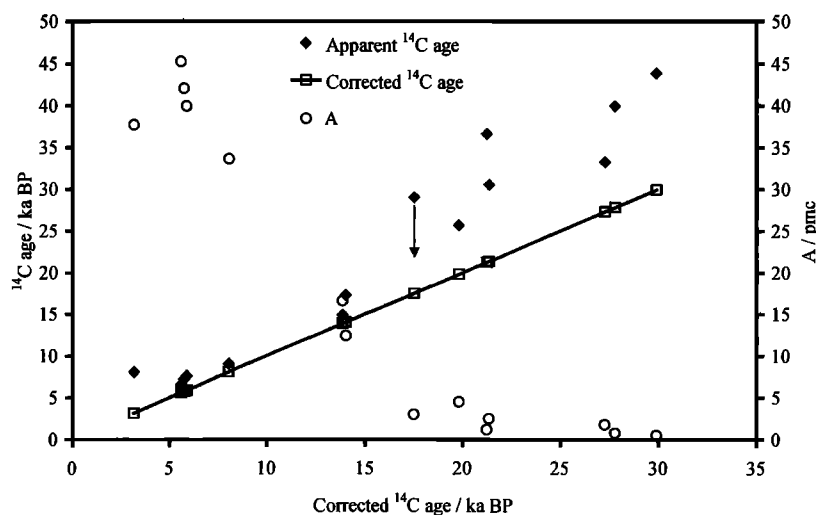


Figure 10. Measured radiocarbon activities (A), apparent radiocarbon ages, equation (28), and corrected radiocarbon ages, equations (28) and (29), with c_{rw} obtained from inverse modeling, case (co,io), plotted versus the corrected radiocarbon age. The arrow indicates the age correction.

appear reasonable and in agreement with the hydrological residence time.

It is tempting to try and interpret the corrected ages of the groundwater samples in terms of climatic history. It is clear that part of the samples have a Holocene age as is indicated by both apparent and corrected ^{14}C age (Figure 10). These samples all have $\delta^{18}\text{O}$ above -6.6‰ . The inverse model with open conditions gives CO_2 pressures of 0.01 to 0.02 atm in the recharge area for these samples. The other samples have conventional ages which range from 13 to 43 ka. The corrected age range is much smaller, however, and spans 12 to 30 ka. The samples have $\delta^{18}\text{O} < -7\text{‰}$, and CO_2 pressures are mostly less than 0.01 atm. It is clear that these waters are representative of the colder climate of the Pleistocene. An interesting aspect would be if the hiatus in the corrected age record could be associated with a lower infiltration rate due to permafrost conditions in the recharge area. In the now available data set, the period of 20 to 25 ka seems to be devoid of samples, and infiltration may have been reduced in this period which corresponds to the latest glacial maximum.

5. Conclusions

It has been shown that inverse modeling of groundwater quality allows one to deduce palaeoconditions in the recharge area. The inverse model must and can account for changes in CO_2 pressure in the recharge area, which are related to climatic conditions and biological production. It was found that Pleistocene samples from the Ledo-Paniselian aquifer in Belgium/Holland have generally lower CO_2 pressures than recent samples. The CO_2 difference is corroborated by lower $\delta^{18}\text{O}$ and is indicative of the colder conditions of the Pleistocene.

The inverse model with variable CO_2 pressure in the recharge area was used to obtain corrected ^{14}C ages for the water samples. The age correction makes the waters up to 15,000 years younger than is indicated by the conventional ^{14}C age.

Acknowledgments. This work forms part of the PALAEAUX-project and has been funded by the European Community as part of the Fourth Framework Programme (Climatology and Natural Hazards). It is contract ENV4-CT95-0156. The authors would like to thank David Parkhurst for making a modification on PHREEQC which facilitated data analyses and for some troubleshooting regarding the "grammar" of the PHREEQC input files. F. J. Pearson and J. E. Landmeyer are thanked for their valuable comments on the manuscript. K. W. acknowledges financial support for the past 15 years from the Fund for Scientific Research Flanders for research on the hydrogeology and hydrogeochemistry of the Ledo-Paniselian aquifer. She is also grateful to M. A. Geyh from the Niedersächsisches Landesamt für Bodenforschung in Hannover, who kindly accepted to perform the isotope analyses in his laboratory.

References

- Appelo, C. A. J., Cation and proton exchange, pH variations, and carbonate reactions in a freshening aquifer, *Water Resour. Res.*, **30**, 2793–2805, 1994.
- Appelo, C. A. J., and D. Postma, *Geochemistry, Groundwater and Pollution*, 536 pp., A. A. Balkema, Brookfield, Vt., 1993.
- Aravena, R., L. I. Wassenaar, and L. N. Plummer, Estimating ^{14}C groundwater ages in a methanogenic aquifer, *Water Resour. Res.*, **31**, 2307–2317, 1995.
- Back, W., B. B. Hanshaw, L. N. Plummer, P. H. Rahn, C. T. Rightmire, and M. Rubin, Process and rate of dedolomitization: Mass transfer and ^{14}C dating in a regional carbonate aquifer, *Geol. Soc. Am. Bull.*, **94**, 1415–1429, 1984.
- Cardenal, J., and K. Walraevens, Chromatographic pattern in a freshening aquifer (Tertiary Ledo-Paniselian aquifer, Flanders-Belgium), *Min. Mag.*, **58A**, 146–147, 1994.
- Cerling, T. E., The stable isotopic composition of modern soil carbonate and its relationship to climate, *Earth Planet. Sci. Lett.*, **71**, 229–240, 1984.
- Cerling, T. E., K. D. Solomon, J. Quade, and J. R. Bowman, On the isotopic composition of carbon in soil carbon dioxide, *Geochim. Cosmochim. Acta*, **55**, 3403–3405, 1991.
- Chapelle, F. H., and L. L. Knobel, Aqueous geochemistry and exchangeable cation composition of glauconite in the Aquia aquifer, Maryland, *Ground Water*, **21**, 343–352, 1983.
- Chapelle, F. H., and L. L. Knobel, Stable carbon isotopes of HCO_3^- in the Aquia aquifer, Maryland: Evidence for an isotopically heavy source of CO_2 , *Ground Water*, **23**, 592–599, 1985.
- Chapelle, F. H., and P. B. McMahon, Geochemistry of dissolved inorganic carbon in a Coastal Plain aquifer, 1, Sulfate from confining beds as an oxidant in microbial CO_2 production, *J. Hydrol.*, **127**, 85–108, 1991.
- Craig, H., The geochemistry of stable carbon isotopes, *Geochim. Cosmochim. Acta*, **3**, 53–92, 1953.
- Degens, E. T., Biogeochemistry of stable carbon isotopes, in *Organic Geochemistry*, edited by G. Eglinton and M. T. J. Murphy, pp. 305–329, Springer-Verlag, New York, 1967.
- Deines, P., D. Langmuir, and R. S. Harmon, Stable carbon isotope ratios and the existence of a gas phase in the evolution of carbonate ground waters, *Geochim. Cosmochim. Acta*, **38**, 1147–1164, 1974.
- Dórr, H., and K. O. Münich, Carbon-14 and carbon-13 in soil CO_2 , *Radiocarbon*, **22**, 909–918, 1980.
- Dudziak, A., and S. Halas, Influence of freezing and thawing on the carbon isotope composition in soil CO_2 , *Geoderma*, **69**, 209–216, 1996.
- Emrich, K., D. Ehhalt, and J. C. Vogel, Carbon isotope fractionation during the precipitation of calcium carbonate, *Earth Planet. Sci. Lett.*, **8**, 363–371, 1970.
- Fontes, J. C., and J. M. Garnier, Determination of the initial ^{14}C activity of the total dissolved carbon: A review of the existing models and a new approach, *Water Resour. Res.*, **15**, 399–413, 1979.
- Halas, S., and A. Dudziak, Precise determination $^{13}\text{C}/^{12}\text{C}$ and CO_2 concentration in minute samples of soil air by mass spectrometry, *Isotopenpraxis*, **25**, 349–351, 1989.
- Hesterberg, R., and U. Siegenthaler, Production and stable isotopic composition of CO_2 in a soil near Bern, Switzerland, *Tellus, Ser. B*, **43**, 197–205, 1991.
- Ingerson, E., and F. J. Pearson Jr., Estimation of age and rate of motion of groundwater by the ^{14}C method, in *Recent Researches in the Fields of Hydrosphere, Atmosphere and Nuclear Geochemistry*, pp. 263–283, Maruzen, Tokyo, 1964.
- Leuenberger, M., U. Siegenthaler, and C. C. Langway, Carbon isotope composition of CO_2 during the last ice age from an Antarctic ice core, *Nature*, **357**, 488–490, 1992.
- Marino, B. D., M. B. McElroy, R. J. Salawitch, and W. G. Spaulding, Glacial-to-interglacial variations in carbon isotopic composition of atmospheric CO_2 , *Nature*, **357**, 461–466, 1992.
- McMahon, P. B., and F. H. Chapelle, Geochemistry of dissolved inorganic carbon in a Coastal Plain aquifer, 2, Modelling carbon sources, sinks and $\delta^{13}\text{C}$ evolution, *J. Hydrol.*, **127**, 109–135, 1991.
- Mook, W. G., On the reconstruction of the initial ^{14}C content of ground water from the chemical and isotopic composition, paper presented at 8th International Radiocarbon Conference, R. Soc. of New Zealand, Wellington, 1972.
- Mook, W. G., The dissolution-exchange model for dating groundwater with ^{14}C , in *Interpretation of Environmental Isotope and Hydrochemical Data in Groundwater Hydrology*, pp. 145–153, Int. At. Energy Agency, Vienna, 1976.
- Mook, W. G., *Principles of Isotope Hydrology*, 153 pp., Free Univ. of Amsterdam, Amsterdam, 1994.
- Mook, W. G., J. C. Bommerson, and W. H. Staverman, Carbon isotope fractionation between dissolved bicarbonate and gaseous carbon dioxide, *Earth Planet. Sci. Lett.*, **2**, 169–176, 1974.
- Parkhurst, D. L., PHREEQC—A computer program for speciation, reaction-path, advective-transport, and inverse geochemical calculations, *U.S. Geol. Surv. Water Resour. Invest. Rep.*, **95-4227**, 143 pp., (with transport addenda by C. A. J. Appelo) 1995.
- Parkhurst, D. L., Geochemical mole-balance modeling with uncertain data, *Water Resour. Res.*, **35**, 1957–1970, 1997.
- Parkhurst, D. L., and C. A. J. Appelo, User's guide to PHREEQC

- (version 2)—A computer program for speciation, batch-reaction, one-dimensional transport, and inverse geochemical calculations, *U.S. Geol. Surv. Water Resour. Invest. Rep.*, 99-4259, 312 pp., 1999.
- Parkhurst, D. L., and L. N. Plummer, Geochemical models, in *Regional Water Quality*, edited by W. M. Alley, pp. 199–225, Van Nostrand Reinhold, New York, 1993.
- Parkhurst, D. L., L. N. Plummer, and D. C. Thorstenson, BALANCE—A computer program for calculating mass transfer for geochemical reactions in ground water, *U.S. Geol. Surv. Water Resour. Invest. Rep.*, 82-14, 29 pp., 1982.
- Pearson, F. J., Jr., and B. B. Hanshaw, Sources of dissolved carbonate species in groundwater and their effects on carbon-14 dating, in *Isotope Hydrology*, pp. 271–286, Int. At. Energy Agency, Vienna, 1970.
- Plummer, N. L., Geochemical modeling—Past, present, future, in *Proceedings of the 7th International Symposium on Water-Rock Interaction, Park City, Utah, 1992*, edited by Y. Kharaka, pp. 23–33, A. A. Balkema, Brookfield, Vt., 1992.
- Plummer, N. L., D. L. Parkhurst, and D. C. Thorstenson, Development of reaction models for ground-water systems, *Geochim. Cosmochim. Acta*, 47, 665–685, 1983.
- Plummer, N. L., J. F. Busby, R. W. Lee, and B. B. Hanshaw, Geochemical modelling of the Madison aquifer in parts of Montana, Wyoming, and South Dakota, *Water Resour. Res.*, 26, 1981–2014, 1990.
- Plummer, N. L., E. C. Prestemon, and D. L. Parkhurst, NETPATH, An interactive code for modelling net geochemical reactions along a flow path version 2.0, *U.S. Geol. Surv. Water Resour. Invest. Rep.*, 94-4169, 130 pp., 1994.
- Reardon, E. J., A. A. Mozeto, and P. Fritz, Recharge in northern climate calcareous sandy soils: Soil water chemical and carbon-14 evolution, *Geochim. Cosmochim. Acta*, 44, 1723–1735, 1980.
- Rightmire, C. T., Seasonal variation in $p\text{CO}_2$ and ^{13}C content of soil atmosphere, *Water Resour. Res.*, 14, 691–692, 1978.
- Rubinson, M., and R. N. Clayton, Carbon-13 fractionation between aragonite and calcite, *Geochim. Cosmochim. Acta*, 33, 997–1002, 1969.
- Thode, H. G., M. Shima, C. F. Rees, and K. V. Krishnamurty, Carbon-13 isotope effects in systems containing carbon dioxide, bicarbonate, carbonate and metal ions, *Can. J. Chem.*, 34, 582–595, 1965.
- Vogel, J. C., Carbon-14 dating of groundwater, in *Isotope Hydrology*, pp. 225–239, Int. At. Energy Agency, Vienna, 1970.
- Vogel, J. C., P. M. Grootes, and W. G. Mook, Isotope fractionation between gaseous and dissolved carbon dioxide, *Z. Phys.*, 230, 225–238, 1970.
- Walraevens, K., Hydrogeology and hydrochemistry of the Ledo-Paniselian in East and West Flanders (in Dutch), Ph.D. thesis, 350 pp., Ghent Univ., Ghent, 1987.
- Walraevens, K., Application of mathematical modeling of the groundwater flow in the Ledo-Paniselian semi-confined aquifer, in *Computer Modeling of Groundwater Flow Problems*, edited by F. De Smedt, *VLIB Hydrol.*, 14, 95–114, 1988.
- Walraevens, K., Hydrogeology and hydrochemistry of the Ledo-Paniselian semi-confined aquifer in east- and west Flanders, *Acad. Anal.*, 52, 12–66, 1990a.
- Walraevens, K., Natural-isotope research on groundwater from the semi-confined Ledo-Paniselian aquifer in Belgium: Application of ^{14}C -correction methods, *Natuurwet. Tijdschr. Ghent*, 72, 79–89, 1990b.
- Walraevens, K., and J. Cardenal, Aquifer recharge and exchangeable cations in a Tertiary clay layer (Bartonian clay, Flanders-Belgium) *Min. Mag.*, 58A, 955–956, 1994.
- Whiticar, M. J., E. Faber, and M. Schoell, Biogenic methane formation in marine and freshwater environments: CO_2 reduction vs. acetate fermentation—Isotope evidence, *Geochim. Cosmochim. Acta*, 50, 693–709, 1986.
- Wigley, T. M. L., Carbon 14 dating of groundwater from closed and open systems, *Water Resour. Res.*, 11, 324–328, 1975.
- C. A. J. Appelo, Valeriusstraat 11, NL-1071 MB Amsterdam, Netherlands. (appt.@xs4all.nl)
- W. J. M. van der Kemp, Sub Atomic Physics Department, Faculty of Physics and Astronomy, Utrecht University, P.O. Box 80.000, NL-3508 TA Utrecht, Netherlands. (kemp@phys.uu.nl)
- K. Walraevens, Laboratory for Applied Geology and Hydrogeology, Ghent University, Krijgslaan 281, B-9000 Ghent, Belgium. (Kristine.Walraevens@rug.ac.be)

(Received June 28, 1999; revised November 18, 1999; accepted December 20, 1999.)